Head Injury Risks and Countermeasures for a Bicyclist Impacted by a Passenger Vehicle

Bengt Pipkorn, Victor Alvarez, Madelen Fahlstedt, Linus Lundin

Abstract The potential injury reducing benefits by a bicyclist helmet and a vehicle mounted bicyclist protection airbag (BPA) was evaluated by means of human body model simulations. The human body model SAFER HBM was positioned on a bicycle and impacted by a passenger vehicle in 40 km/h. Three conditions were evaluated; without countermeasure, with helmet and helmet together with bicyclist protection airbag (BPA). Head injury risk was evaluated by means of predicted HIC15, BrIC and strain in the brain.

The impact conditions caused different impact points on the vehicle, windscreen and A-pillar. Both the impact points showed highest HIC and peak brain tissue strain for the case with no countermeasures and lowest values when including both the helmet and BPA. BrIC increased when including the BPA for the windshield impact where the head did not impact the BPA, but a reduction was observed when the impact location was at the A-pillar.

Generally head injury risk was reduced for a bicyclist wearing a helmet when impacted by a passenger vehicle in 40km/h. Additional reductions was obtained for a vehicle with a BPA. Therefore, the conclusion from this study was that helmet and BPA have the potential to protect the head in vehicle to bicyclist impacts.

Keywords bicyclist, bicyclist protection airbags, head injury, helmet, vulnerable road user

I. INTRODUCTION

In 2016 in the European Union 2015 bicyclists were killed in road crashes which accounts for a decrease by 24% since 2000 [1]. Since 2010 the number of bicyclist fatalities in the EU is stagnating. In Sweden bicyclists account for a higher proportion of causalities than any other road user type [2]. In the Netherlands, US and Sweden, most bicyclist crashes are single cycle crashes [3–5] and about 17% of bicyclist crashes involved motor vehicles [6]. The most common bicyclist to vehicle crash configurations are 'car front to bicyclist side', 'cyclist front to car side', 'car front to bicyclist front' and 'dooring' in that order [6]. The body parts with the highest risk for serious injuries were the legs and head with 39% and 38% injury risk respectively followed by the chest with 32% [7]. The three most frequent head impact locations were the A-Pillar with 37% followed by the glass (windscreen) and roof edge with 26% each [7]. The head-to-windshield injury mechanism was most common while chest-to-hood, chest-to-windshield and head-to-ground were more or less equally frequent combinations. The vehicle impact speed has been found to be at average from 20-36km/h [6–8], but with a large variation up to 70km/h, and bicycle velocity of 15km/h [8].

The protective effect of bicycle helmets has been evaluated both with epidemiological studies (e.g., [9–12], experimental tests (e.g., [13-14]) and computer simulations (e.g., [15-16]). There are several studies that have evaluated the protective effect of the helmet in vehicle impacts. Mizuno et al. [17] evaluated the protective effect of the helmet against the vehicle front. They shoot pedestrian head form against different parts of the vehicle and found a reduction of HIC when wearing a helmet if the impact was against the A-pillar, hood or roof header but an increase in HIC if the impact was against the windscreen. A similar study was performed by Matsui et al. [18]. They found the largest reduction of HIC when wearing a helmet if the impact was against the roof side rail and lowest reduction when impacting the center of the hood. Ito et al. [19] studied A-pillar impact with finite element models and found that the helmet can reduced the risk of skull fracture and decrease the brain tissue strain but also showed that the helmet foam could bottom out in some impact situations.

Another way to protect the body in a bicyclist-to-vehicle crash is by having airbags outside the vehicle. Some previous studies, e.g. [20], have shown a decrease of HIC when a pedestrian is hit by a vehicle equipped with a pedestrian airbag compared to not equipped with an airbag. However, an evaluation of rotationally based injury

B. Pipkorn (e-mail: bengt.pipkorn@autoliv.com; tel: +46 (0)322 626341) is Adjunct Professor at Chalmers University of Technology, Gothenburg, and Director of Simulation and Active Structures at Autoliv Research, Vårgårda, Sweden. V. Alvarez is a researcher at Lightness by Design contracted by Autoliv. M. Fahlstedt is researcher at KTH Royal Institute of Technology in Stockholm, L. Lundin is a contractor at AFRY.

measures has not been included in the previous studies. An airbag system was presented with the potential to protect both pedestrians and bicyclists [21]. However, bicyclists with helmets were not addressed in the study. Therefore, since bicycle helmets are frequently used today there is a need include helmets in the evaluation of bicyclist protection airbags (BPA).

For evaluation of bicycle safety, a validated human body model seems to be an applicable tool. In recent years, mathematical human body models (HBMs), including finite element (FE) HBMs, have been developed to complement mechanical anthropometric test devices (ATDs) as an evaluation and development tool for protection system assessments. The HBM has several advantages in these tasks compared to the ATD. The HBM is omnidirectional by design and can therefore predict human kinematics and injury risk for all loading directions. The FE-HBMs have a detailed representation of the human anatomy and material properties. In the HBM the injury risk can be evaluated for specific anatomical structures, which makes it possible to address injury at a detailed level, such as at a tissue level. These models enable evaluation of physical variables mechanically related to injury, e.g. energy and strain [22-23]. Today, there are several HBMs representing average-sized male occupants, of which the two most popular HBMs are the Total Human Model for Safety (THUMS) AM50 [24] and the Global Human Body Model Consortium (GHBMC) M50-O [25]. An additional human body model, the SAFER HBM version 9 model comprise detailed head and chest models developed and validated for tissue level injury prediction [26-27]. A detailed description of the model can be found in Appendix A. The head model has been validated against several localised brain motion, intracerebral acceleration and intracranial pressure experiments [28-29]. A more detailed description and material properties can be found in Appendix B. The maximal principal Green-Lagrange strain in the brain was chosen as a predictor of CNS (Central Nervous System) injuries since it has been shown to correlate with diffuse axonal injuries [30–33] as well as for mechanical injury to the blood-brain barrier [34]. As the brain is sensitive to rotational motion due to its low shear modulus [35–37] it is also important to capture the motion of the head correctly. This emphasises the importance to model all boundary conditions to the head in as detailed a manner as possible and the need for a windscreen model that can capture both accelerations and deformations correctly.

Due to the composite structure the vehicle windscreens, which is two layers of glass and a thin interlayer of polyvinyl butyral (PVB), attains a relatively complex pattern of failure. A variety of approaches have been employed to capture this behaviour in FE models for dynamic explicit solvers, from solely detailed 3D solid elements representing each layer, both in blast [38-39] and impact applications [40-41] to a combination of shell elements and solid elements [42]. In a modelling approach modelling a windscreen with three shell layers, representing the glass and PVB, separated by the distance of their thickness, using a non-local failure criterion to initiate fracture in the glass, it was found that the model was able to capture both accelerations and deformations of a head-like impact to a windscreen, with a maximum error of about 18% in acceleration and even less in deformation [43]. The aim of the study is to evaluate the injury pattern and the potential injury reducing benefits of a bicycle helmet and an inflatable restraint system for a bicyclist impacted by a passenger vehicle.

II. METHODS

The human body model SAFER HBM v9 was positioned as a bicyclist on a generic deformable bicycle model developed in the APROSYS project [44] (Fig 1). The generic bicycle model comprised a frame, handlebar, pedals wheels with spokes and a seat pan. The bicycle and human body model were impacted by a Honda Accord MY 2013 available from the NHTSA database [45]. The model was simplified by removing deformable parts in the interior of the vehicle that would not interact with the HBM and replaced with equivalent inertia and mass. The windscreen of the original Honda Accord model was replaced by a previously developed and validated detailed model of the windscreen that included a failure model [43]. All simulations were solved with LS-DYNA mpp s R9.3.1, Revision 140922 using 16 computational nodes. No breaking was applied to the vehicle and the coefficient friction between the bicycle, bicyclist, ground and vehicle was set to 0.3.

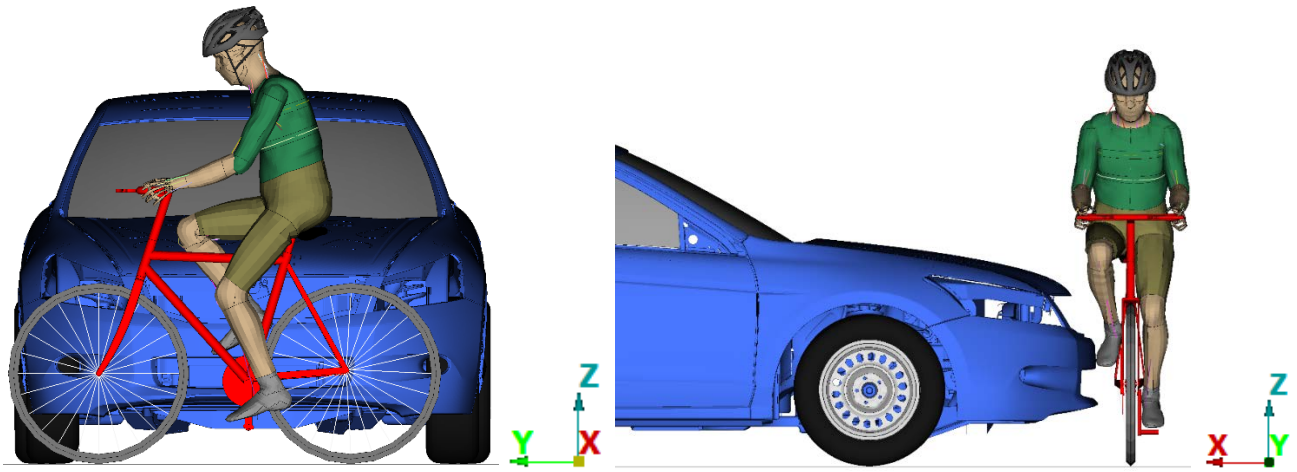

Fig. 1. SAFER HBM positioned on the bicycle model from the APROSYS project.

Two different impact scenarios were evaluated (Fig. 2):

1. Bicycle is standing still and impacted on the side by the vehicle travelling at 40km/h
2. Bicycle is travelling at 15km/h impacted on the side by the vehicle travelling at 40km/h

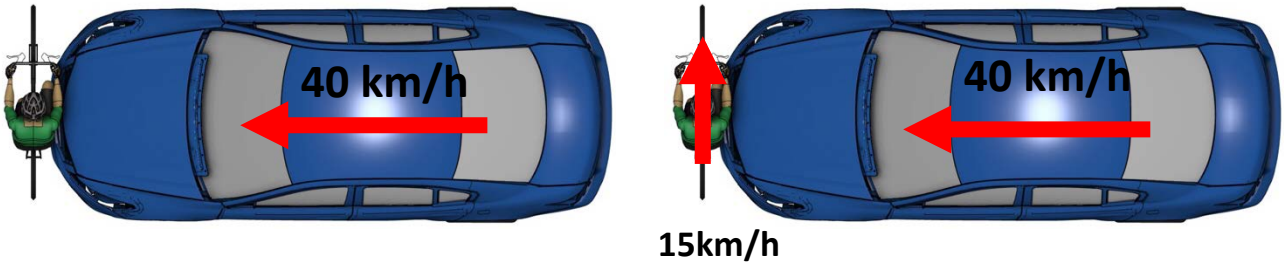

Fig. 2. Bicycle to passenger vehicle crash configurations; stationary bicyclist (left) and travelling in 15 km/h (right)

The injury risk for the bicyclist was evaluated both with and without helmet and with and without inflatable protection system (Fig 3). The helmet model was developed and validated by Fahlstedt et al. [16]. Good correlation between the prediction from the helmet model and corresponding mechanical tests (radial and oblique) was obtained [16]. A coefficient of friction of 0.3 was used between the head and helmet liner, corresponding to measurements from PMHS experiments between head and helmet liner material [46]. The inflatable protection system was a prototype bicyclist protection airbag (BPA) developed for protection of bicyclists in a passenger vehicle to bicyclist impact. The wrap around distance (WAD) of the bag was 2800mm which is greater than for a pedestrian airbag. The BPA was covering the lower part of the windscreen and a significant portion of the A-Pillar (Fig. 4). The inflatable restraint was combined with a hood lifter system which lifted the hood 190mm when the bag was inflated. When inflated the thickness of the BPA was 250mm and the pressure was 25kPa. The bag comprised of two sections covering each A-Pillar. Width of one of the sections that cover the A-pillar was approximately 300mm. The bag was inflated at the start of the simulation. In total six different configurations were evaluated. They are presented in Table I.

Fig. 3. Helmet (left) and bicyclist airbag (right)

TABLE I
Evaluated Impact Configurations

Simulation	Vehicle Velocity [km/h]	Bicyclist velocity [km/h]	Countermeasure
1	40	0	No
2	40	0	Helmet
3	40	0	Helmet + BPA
4	40	15	No
5	40	15	Helmet
6	40	15	Helmet + BPA

Head AIS2+ injury risk was assessed by HIC15, BrIC [47] and strain in the brain. For BrIC, the injury risk curve based on CSDM was used [47], and for HIC the risk curve from NHTSA [48]. To assess injury risk from strain in the brain the peak value of the first principal Green-Lagrange (G-L) strain of the brain tissue was extracted from the head model. Based on the strain prediction, the brain injury risk was calculated with risk curves developed based on previously published principle and data [28][49], but adapted for AIS2 level injury. Accelerations and angular velocities of the head were all measured in head local coordinate system in accordance with SAE standard sign convention.

III. RESULTS

For the bicyclist with 0km/h velocity (stationary) the head impacted close to the center of the windscreen while for the bicyclist with 15km/h velocity the head impacted the A-Pillar of the vehicle (Fig 4). For both impact locations the wrap around distance was similar, about 2400mm, but the transverse offset was larger for the bicyclist with 15km/h velocity. Figures of the HBM at time of head impact can be found in Appendix C. The windshield was fractured in all impact configurations except for the moving bicyclist impacted by a vehicle with BPA (Fig C1 and C2).

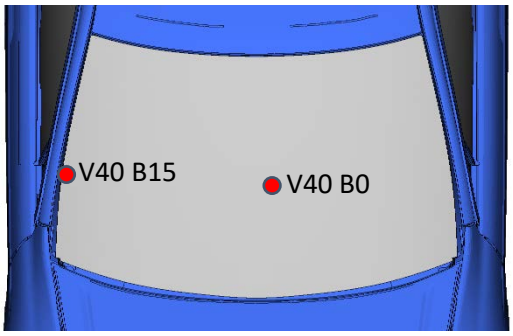

Fig. 4. Approximate head impact points on windscreen for all impact configurations. “V” indicates vehicle velocity and “B” bicycle velocity (km/h)

Head Impact Velocity

For the resultant linear head impact velocity relative to the moving vehicle, there was 16 km/h difference between the highest and lowest impact velocity. Highest head impact velocity was 48km/h. It was for the stationary bicyclist wearing a helmet (Table II). The lowest head impact velocity was 32km/h, for the bicyclist without helmet and the bicyclist crossing the path of the vehicle at 15km/h. Plots of the resulting relative head velocity vs time can be found in Appendix D

TABLE II
Resulting Relative Head Impact Velocity

Bicyclist Velocity (km/h)	Countermeasure	Head Impact Velocity (km/h)
0 (Stationary)	No	46
	Helmet	48
	Helmet and BPA	41
15	No	32
	Helmet	35
	Helmet and BPA	34

Head Linear Acceleration and Rotational Velocity

For both the stationary bicyclist and the bicyclist travelling at 15km/h, peak resulting linear acceleration was highest for the bicyclist without helmet (Fig 5a). For the bicyclist wearing a helmet, peak linear acceleration was reduced and for the combination of helmet and BPA head resulting acceleration was reduced even more in both impact configurations.

For the stationary bicyclist greatest resulting head angular velocity was for the bicyclist wearing a helmet impacted by a vehicle with a BPA (Fig 5b). The peak resulting angular velocity was similar with and without helmet in the same impact configuration. For the bicyclist travelling at 15km/h greatest resulting head angular velocity was for the bicyclist without helmet. For the bicyclist wearing a helmet peak resulting angular velocity was reduced and for the combination of helmet and BPA head resulting angular velocity was reduced even more for both impact configurations. The angular velocity over time is shown in Appendix E.

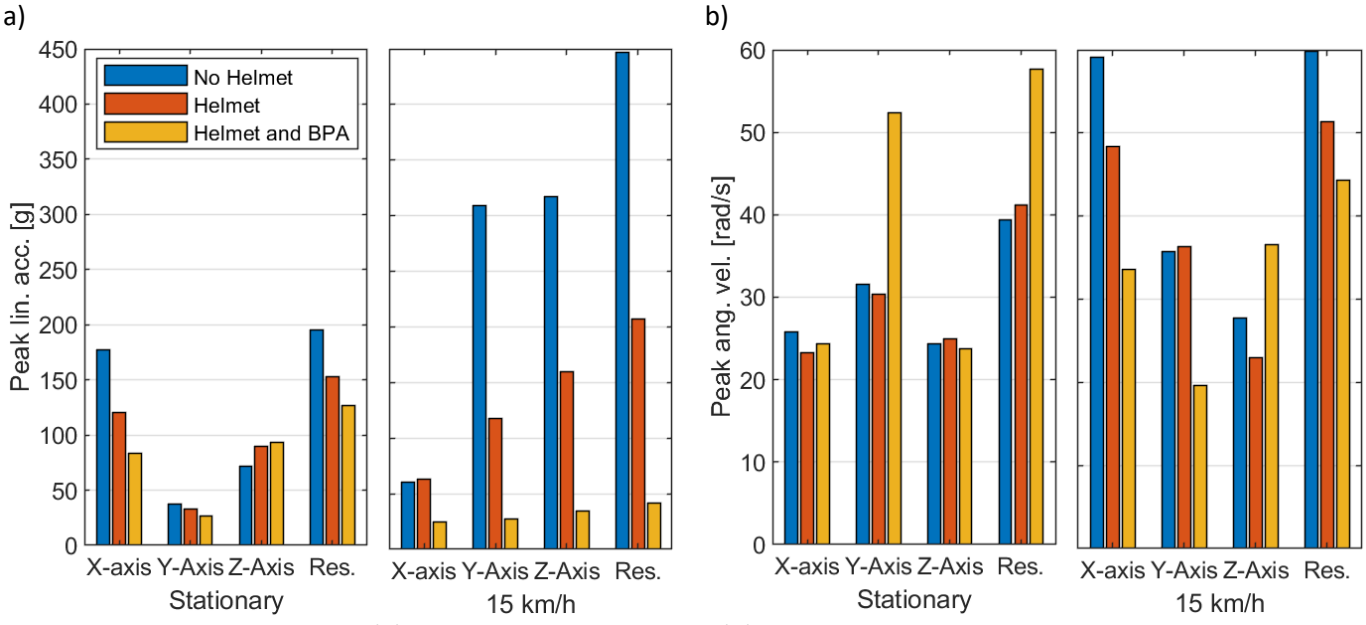

Fig. 5. Peak linear acceleration (a) and peak angular velocity (b)

HIC, BrIC and Strain

For the stationary bicyclist and the bicyclist travelling at 15km/h greatest HIC15 value was for the bicyclist without helmet. For the bicyclist wearing a helmet HIC15 was reduced and for the combination of helmet and BPA head resulting acceleration was reduced even more for both impact configurations (Fig 6).

Greatest BrIC value for the stationary bicyclist was for the bicyclist wearing a helmet impacted by a vehicle with a BPA while lowest was for the bicyclist wearing a helmet only (Fig 6). For the bicyclist travelling at 15 km/h

greatest BrIC value was for the bicyclist without helmet. For the bicyclist wearing a helmet BrIC was reduced and for the combination of helmet and BPA head BrIC was reduced even more (Fig 6).

Greatest strain in the brain for the stationary bicyclist was for the bicyclist wearing a helmet (Fig. 6). Lowest was for the bicyclist wearing a helmet impacted by a vehicle with a BPA. However, the differences were small. For the bicyclist travelling at 15 km/h greatest strain was for the bicyclist without helmet. For the bicyclist wearing a helmet strain in the brain was reduced and for the combination of helmet and BPA the strain in the brain was reduced even more for both impact configurations (Fig 6). The time histories for the strain in the brain can be seen in Appendix F.

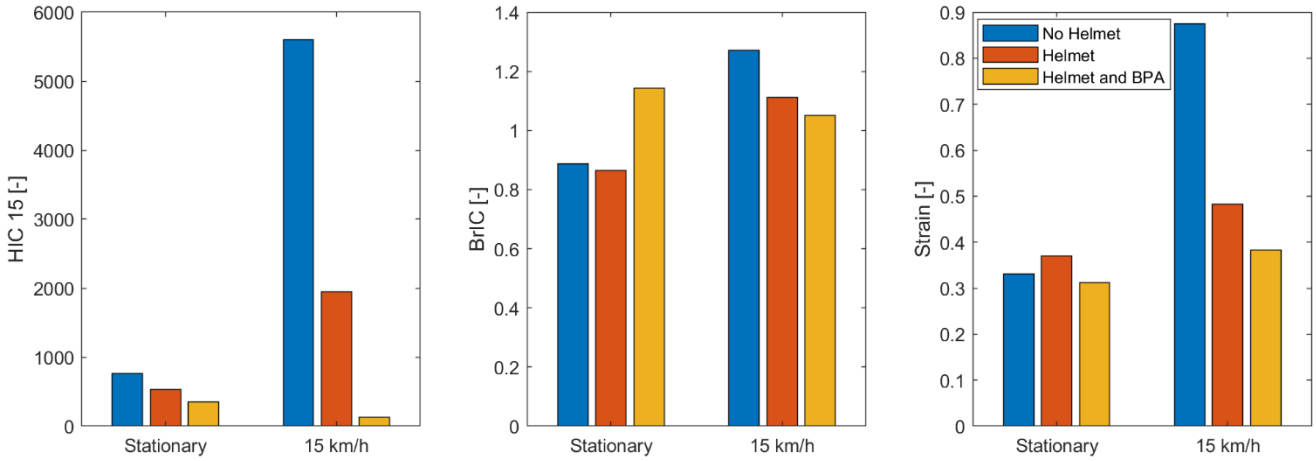

Fig. 6. HIC15, BrIC and strain in the brain for stationary and bicyclists travelling at 15km/h with No helmet, helmet and helmet plus BPA.

Head Injury Risk

For the stationary bicyclist a 72% risk for an AIS2+ head injury was predicted by HIC15 for the bicyclist without helmet (Fig. 7). The AIS2+ injury risk was reduced to 43% for the bicyclist wearing a helmet and 20% for the bicyclist wearing a helmet impacted by a vehicle with a BPA. BrIC predicted 71% head injury risk for the bicyclist without helmet. For the bicyclist with helmet head injury risk was reduced to 67% while for the bicyclist with helmet impacted by a vehicle with BPA, the predicted head injury risk was increased to 96%. The strain in the brain predicted a 22% AIS2 head injury risk for the bicyclist without helmet. For the bicyclist with helmet, the predicted AIS2 head injury risk was increased to 28% and for the bicyclist with helmet impacted by a vehicle with BPA, the predicted AIS2 head injury risk was reduced to 19%.

For the bicyclist travelling at 15km/h a 100% AIS2+ head injury risk was predicted by HIC15 for the bicyclist without helmet and with helmet (Fig. 7). For the bicyclist wearing a helmet and travelling at 15km/h, head injury risk was reduced to 3% when impacted by a vehicle with a BPA. BrIC predicted a 99% head injury risk for the bicyclist without helmet. For the bicyclist with helmet head injury risk was reduced to 95% and for the bicyclist with helmet impacted by a vehicle with BPA, the predicted head AIS2+ injury risk was reduced to 91%. The strain in the brain predicted a 97% AIS2 injury risk for the bicyclist without helmet. For the bicyclist wearing a helmet head injury risk was reduced to 52% and for the bicyclist wearing a helmet impacted by a vehicle with a BPA, predicted head injury risk was reduced to 31%.

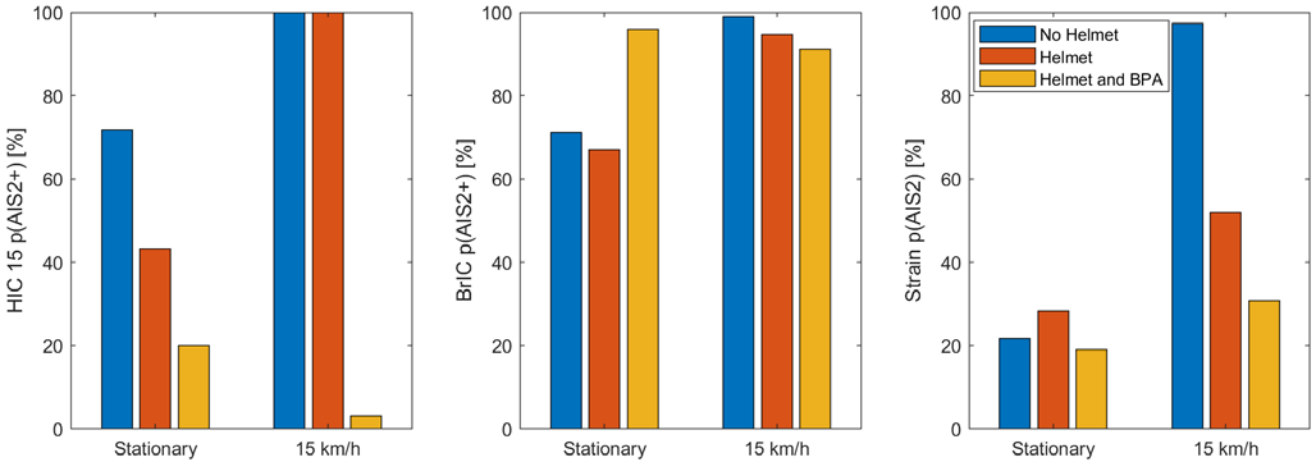

Fig. 7. AIS2 risk based on; HIC15, BrIC and Strain in the brain for stationary and bicyclists travelling at 15km/h with No helmet, helmet and helmet plus BPA.

IV. Discussion

The aim of this study was to evaluate the injury pattern and the potential injury reducing benefits of bicycle helmets and inflatable restraint system for a bicyclist impacted by a passenger vehicle. One impact configuration was a stationary bicyclist impacted by a passenger vehicle at 40km/h. Another impact configuration was a bicyclist travelling at 15km/h impacted by a passenger vehicle at 40km/h. 40km/h impact velocity was used due to the fact that it is used in the Euro NCAP rating procedure [50] for head impacts and it is close to the average impact velocity in the field [6-8]. The different impact configurations resulted in different head impact points and velocities. Head impact point for the stationary bicyclist was in the middle of the windscreen while for the bicyclist travelling at 15km/h the head impacted the A-Pillar. Head impact velocity varied from 32km/h to 48km/h.

The relative velocity between the head and the vehicle was reduced when the HBM was in contact with the vehicle. The longer time the HBM was interacting with the vehicle before head impact, the lower was the relative impact velocity of the head. Most of the velocity from the vehicle is transferred to the head as vertical velocity (i.e. the velocity towards the ground, or z-direction), before head impact. But the friction between the HBM and vehicle also gives the head velocity in the same direction as the traveling direction of the vehicle (the negative x-direction) before head impact. After the HBM has impacted the windscreen, this is also the main velocity component of the whole HBM. As can be seen in Fig. D1, the resulting relative head velocity is slightly altered between no helmet and helmet condition, possibly due to the slightly altered inertia of the helmet. But more importantly, the head contact with the windscreen occurs earlier for the helmeted condition, mostly due to the additional 30mm thickness of the helmet, giving less time for the relative velocity to be reduced. This results in a 2 km/h lower impact velocity for the un-helmeted condition. In the case of the vehicle with the BPA, the relative head velocity starts to be reduced earlier than in the two other cases. This can be explained by the fact that the hood has a higher angle against the HBM, due to the lifted hood, increases the interaction between the vehicle and HBM. In addition, the HBM impacts the BPA with the upper part of the shoulder, that sinks in to the BPA, which acts to drag the HBM in the direction of the moving vehicle before the head impacts. This results in an additional reduction of head impact velocity.

Generally, head impact velocity was lower for the bicyclist travelling at 15km/h (Fig. D2). This is explained with the same basic principles as described above, in combination with the fact that the arm of the HBM has altered kinematics, causing the elbow to impact the windscreen, and hence transferring more vehicle velocity in the direction of travel to the HBM, before head impact. The HBM also travels a slightly longer distance than in the stationary conditions, giving a later head impact and more time for the velocity to be reduced. In this configuration, the BPA does, however, not give the lowest impact velocity, although it can be seen in Fig. D2 that the head relative velocity is reduced earlier and more, than without the BPA, as for the stationary configurations. The difference in the configuration with the 15 km/h bicyclists velocity from the stationary one, is that the HBM impacts with the head directly to the BPA, causing a much earlier head contact, and as a result, an increase of 2 km/h head impact velocity from the un-helmeted configuration to the helmeted with the BPA.

All injury metrics showed significantly higher injury risk for A-Pillar impacts, compared to windscreen impacts. This was in agreement with the findings of another HBM study in which it was found that both HIC and cumulative

strain damage (CSDM) were significantly higher in A-Pillar impacts than in windscreen impacts [51]. A significant reduction of the peak linear acceleration and HIC15 was obtained for a bicyclist wearing a helmet impacted by a vehicle without and with a BPA. However, the reduction was less pronounced for the windscreen impact compared to the A-pillar impact. For the windscreen impact, the windscreen fractured and absorbed part of the impact energy for the bicyclist with and without helmet. For the A-Pillar impact all energy was absorbed by the helmet and helmet and BPA. The reduction in HIC value was partly contradictive to the results Mizuno et al. [17]. In the study by Mizuno no reduction for helmet impacts against the windscreen was obtained. However, reduction of HIC when impacting the A-pillar was obtained. The reduction in HIC15 for bicyclists with a helmet impacting the A-Pillar is supported by the study by Matsui et al. [18].

For the stationary bicyclist impacting the windscreen, the peak angular velocities were caused by a combination of helmet and BPA. The increase was mainly around the y-axis of the head. The BPA was impacted by the upper back before there was a windscreen to head impact (Appendix C). A rotation of the head around the y-axis was introduced by the back to BPA impact. The increase in BrIC and peak angular velocity was not observed for the peak strain of the brain tissue. Similar strain levels were generated for the bicyclist with and without helmet impacted by a vehicle with and without BPA. The lack of reduction of peak strain when introducing countermeasures for the windscreen impact can be due to the resulting low stiffness of the windscreen after fracture of the glass. It was also observed that the maximum strain in the brain was not correlating with the time of impact for the stationary bicyclist, with and without helmet (152-154ms) (Fig F1).

Although the strain in the brain was significant from the initial head to windscreen impact, the peak strain value occurred when the fractured windscreen was stretched out and the rebound of the head was initiated (208 ms). Hence, the maximum strain in the brain seems to come from the induced rotational motion caused by the interaction between the head/helmet and the windscreen. For the bicyclist wearing a helmet, peak strain was occurring at a similar point in time as without helmet. The liner of the helmet was compressed approximately 10mm up to windscreen fracture. For the stationary bicyclist impacted by a vehicle with a BPA, the peak strain in the brain was after the initial head-to-windscreen contact (164ms). There was however, also in this case significant strain in the brain at the time of head rebound (218ms). A possible explanation why this last peak strain was smaller than without the BPA can be that the BPA was increasing the distance between the head and windscreen, reducing the distance the head can be pushed into the fractured windscreen, inducing less rotational motion to the head.

For the bicyclist travelling at 15km/h, in which there was a head to A-Pillar impact, resultant peak angular velocity and BrIC were reduced for the bicyclist wearing a helmet. The peak angular velocity and BrIC were reduced even more when the impacting vehicle was equipped with a BPA. However, the angular velocity around y-axis was reduced and angular velocity around z-axis was increased when the BPA was added. The interaction between the head and the A-Pillar and the head and the BPA were significantly different therefore differences in head angular velocity can be expected. The same strain pattern was observed for peak strain as for peak resultant angular velocity. It can be seen in Fig. E2 that the maximum peak strain in the brain for the impact with the BPA was late in impact (229ms), after the head rebound from BPA.

Greatest injury risk reduction for helmet and BPA was when injury risk was assessed by the strain in the brain. Greatest reductions were observed for the A-Pillar impacts. The injury risk for A-Pillar impacts was significantly greater than for the windscreen impacts. Even for the A-Pillar impact when the bicyclist was protected by a helmet and a BPA the injury risk was greater than for all windscreen impacts. It was shown by Fredriksson et al. [8] that many of the head impacts in bicycle accidents are close to the frame of the windscreen and not at the center. Therefore, it is important to also include impacts to the windscreen frame when evaluating bicycle safety.

Injury risk curves were used for HIC, BrIC and strain in the brain to assess injury risk. Different injury mechanisms are addressed by the different risk curves. Different injury risk was predicted by the different injury measures. A decrease for the stationary bicyclist was predicted by HIC for the bicyclist wearing a helmet and impacted by a vehicle with a BPA. The same reduction in risk was not predicted by BrIC or strain. In previous studies [52] it was found that HIC and linear acceleration were more associated with skull fracture than brain injuries. The results suggest a low risk for skull fracture, especially for the A-pillar when including the BPA and helmet. It was also observed that BrIC predicted a higher injury risk. This can partly be explained by the fact that the BrIC injury risk curve used was for AIS2+, whereas the injury risk curve developed for the strain in the brain was for AIS2. The strain-based injury risk curve was based non-injured and concussion cases.

The limitation of the study was that only one vehicle model, one helmet design and one BPA design were evaluated. The helmet model used was a model of a state-of-the-art bicycle helmet that is used by numerous bicyclists on the road today. The vehicle model used was a model of a common vehicle sold globally. The BPA was a model of a prototype BPA. Therefore, the components were considered adequate for the study carried out.

One impact velocity of the vehicle was used, and 0km/h or 15km/h were applied to the bicyclist. Altering the bicyclist speed would alter the impact point on the vehicle. However, two common impact point on the vehicle front were evaluated in the study. In this study three different configurations were used no countermeasure, including a helmet and including both helmet and BPA. The helmet use varies among different countries and even between different regions in the country [53]. Therefore, a future study evaluating bicyclist to BPA impact for a bicyclist not wearing a helmet seems applicable. Another limitation was that influence of muscle activation on the bicyclist kinematics was not included in the study. Active muscles can alter the impact velocity and impact point of the head due to the bicyclists using the arms to limit the impact speed to the vehicle. However, in pedestrian evaluations it was shown using an active model that the influence of muscle activation was small on pedestrian kinematics and injury risk in vehicle impacts [54-55].

The focus of this study was injuries caused by the impacts to the vehicle, however, a large portion of head injuries are likely also caused by ground impacts [7][21]. The simulation with bicyclist velocity of 15km/h and using a helmet was extended to include ground impact (Fig. 8). The strain in the brain for this simulation was included in Fig. F3 and shows an almost 3 times higher peak in strain for the ground impact compared to the vehicle impact. Head to ground impact velocity was 12.4m/s. However, the ground was modeled as infinitely stiff and the HBM impacts the head/helmet first to the ground and can hence be considered an overestimation and worst-case scenario. It should also be noted that the simulation has a duration of about 1s with several laps of rotation of the HBM before ground impact, both aspects that can affect the accuracy in explicit FE-simulations. It was also observed that the impact point on the helmet was at the same impact point as the impact to the A-pillar. Therefore, the helmet was already deformed before impacting the ground. Reduced protective benefits of the deformed helmet can be expected.

Fig. 8. Ground impact from bicyclist travelling at15 km/h with helmet.

Today's helmets are evaluated against a hard surface, either flat or curbstone, in the helmet test standard [56–58]. This implies that the helmet should be more optimized against A-pillar impacts, but the test standard and the simulated impacts in this study differs in several aspects. In the helmet test standard, the impact is radial in lower impact velocity and only a representation of the head is included in the tests. Nevertheless, the results indicate that the helmet show a more expected result in reducing the injury risk, with all used injury metrics, in the impacts towards the A-pillar. Although the helmet has a clear reduction of injury risk for the impact against the A-pillar, it could be considered still relatively high, with a 52% risk of AIS2, and hence a benefit of including the BPA, reducing the risk down to 31%. On the other hand, the impact towards the windscreen seems to generate a loading condition not fully considered in the development of helmets. Although the predicted injury level for the windscreen impacts was lower than the A-pillar impacts, it can also be considered relevant to better understand the injury mechanisms, and further develop protective systems to also reduce the injuries caused by windscreen impacts.

In the study a prototype BPA was evaluated. However other countermeasures exist, potentially addressing mitigating head injuries [59]. In addition, it is known that autonomous emergency braking (AEB) and BPA complement one another in reducing injury risk [21]. Other countermeasures are speed reduction, friendlier car design (perhaps incl. BPA) [60].

It was found that the BPA was an effective countermeasure in reducing head injury risk for bicyclists wearing a helmet. It can be assumed that the BPA is an even more effective countermeasure for bicyclists not wearing a helmet impacted by a vehicle. Future evaluation will be carried out evaluating the BPA benefits for bicyclists not wearing a helmet when impacted by a passenger vehicle.

V. CONCLUSIONS

A helmet reduces head injury risk for a bicyclist impacted by a passenger vehicle. Additional reduction in injury risk can be achieved by a BPA mounted on the vehicle.

VI. ACKNOWLEDGEMENT

The project was carried out at SAFER – Vehicle and Traffic Safety Centre at Chalmers, Sweden, and financed by FFI (Strategic Vehicle Research and Innovation), by VINNOVA, the Swedish Transport Administration, the Swedish Energy Agency and the industrial partners. The project partners are KTH - Royal Institute of Technology, Autoliv Research, Volvo Cars, MIPS and POC.

VII. REFERENCES

[1] Traffic Safety Basic Facts, 2018.

[2] Berg, Y, Analys av trafiksäkerhetsutvecklingen 2011, Målstyrning av trafiksäkerhetsarbetet mot etappmålen 2020, 2012.

[3] Schepers, P , Agerholm, N , et al., An international review of the frequency of single-bicycle crashes (SBCs) and their relation to bicycle modal share, *Injury Prevention*, 2015, 21:e138–e143.

[4] Stutts, JC , Hunter, WW, Motor vehicle and roadway factors in pedestrian and bicyclist injuries: An examination based on emergency department data, *Accident Analysis and Prevention*, 1999, 31(5):505–514.

[5] Thulin, H , Niska, A, Tema Cycle - injured bicyclists. Analysis based on hospital registered injury information from STRADA, 2009.

[6] Lindman, M , Jonsson, S , et al., Cyclists interacting with passenger cars; a study of real world crashes, Proceedings of *The International Research Council on Biomechanics of Injury (IRCOBI) Conference*, 2015.

[7] Fredriksson, R , Rosén, E, Priorities for Bicyclist Protection in Car Impacts – a Real life Study of Severe Injuries and Car Sources, Proceedings of *the IRCOBI Conference*, 2012.

[8] Zander, O , Hamacher, M, Revision of Passive Pedestrian Test and Assessment Procedures to Implement Head Protection of Cyclists, Proceedings of *25th International Enhanced Safety of Vehicles (ESV) Conference*, 2017.

[9] Thompson, D , Rivara, F , Thompson, R, Helmets for Preventing Head and Facial Injuries in Bicyclists (Review), *Cochrane Database of Systematic Reviews*, 1999, 4:1–29.

[10] Curnow, WJ, The Efficacy of Bicycle Helmets Against Brain Injury., *Accident Analysis & Prevention*, 2003, 35(2):287–292.

[11] Amoros, E , Chiron, M , Martin, J-L , Thelot, B , Laumon, B, Bicycle Helmet Wearing and the Risk of Head, Face, and Neck Injury: a French Case-Control Study Based on a Road Trauma Registry, *Injury Prevention*, 2012, 18:27–32.

[12] Bambach, MR , Mitchell, RJ , Grzebieta, RH , Olivier, J, The Effectiveness of Helmets in Bicycle Collisions with Motor Vehicles: A Case-Control Study, *Accident Analysis & Prevention*, 2013, 53:78–88.

[13] McIntosh, AS , Lai, A , Schilter, E, Bicycle Helmets: Head Impact Dynamics in Helmeted and Unhelmeted Oblique Impact Tests, *Traffic Injury Prevention*, 2013, 14(5):501–508.

[14] Cripton, PA , Dressler, DM , Stuart, CA , Dennison, CR , Richards, D, Bicycle Helmets are Highly Effective at Preventing Head Injury During Head Impact: Head-Form Accelerations and Injury Criteria for Helmeted and Unhelmeted Impacts, *Accident Analysis and Prevention*, 2014, 70:1–7.

[15] McNally, DS , Whitehead, S, MADYMO Simulation of Children in Cycle Accidents: A Novel Approach in Risk Assessment, *Accident Analysis & Prevention*, 2013, 59:469–478.

[16] Fahlstedt, M , Halldin, P , Kleiven, S, The Protective Effect of a Helmet in Three Bicycle Accidents - A

Finite Element Study, *Accident Analysis and Prevention*, 2016, 91:135–143.
[17] Mizuno, K , Ito, D , et al., Adult Headform Impact Tests of Three Japanese Child Bicycle Helmets into a Vehicle, *Accident Analysis & Prevention*, 2014, 73:359–372.
[18] Matsui, Y , Oikawa, S , Hosokawa, N, Effectiveness of wearing a bicycle helmet for impacts against the front of a vehicle and the road surface, *Traffic Injury Prevention*, 2018, 19(7):773–777.
[19] Ito, D , Yamada, H , Oida, K , Mizuno, K, Finite Element Analysis of Kinematic Behavior of Cyclist and Performance of Cyclist Helmet for Human Head Injury in Vehicle-to-Cyclist Collision, Proceedings of *Proceedings of the International Research Council on Biomechanics of Injury (IRCOBI) Conference*, 2014.
[20] Lim, JH , Park, JS , Yun, YW , Jeong, SB , Park, GJ, Design of an airbag system of a mid-sized automobile for pedestrian protection, *Proceedings of the Institution of Mechanical Engineers, Part D: Journal of Automobile Engineering*, 2015, 229(5):656–669.
[21] Fredriksson, R , Ranjbar, A , Rosen, E, Integrated Bicyclist Protection Systems - Potential of Head Injury Reduction Combining Passive and Active Protection Systems, Proceedings of *The 24th Enhanced Safety Vehicle (ESV) Conference*, 2015, (Paper Number 15-0051):
[22] Rouhana, SW , Bedewi, PG , et al., Biomechanics of 4-Point Seat Belt Systems in Frontal Impacts, *Stapp Car Crash Journal*, 2006, 47:367–399.
[23] Trosseille, X , Baudrit, P , Leport, T , Vallancien, G, Rib Cage Strain Pattern as a Function of Chest Loading Configuration, *Stapp Car Crash Journal*, 2008, 52(November):205–231.
[24] Human Body Models for Injury Analysis THUMS®, *Toyota Central R&D Labs. INC.* [Online]. Available: https://www.tytlabs.com/tech/thums/index.html. [Accessed: 26-Nov-2018].
[25] Virtual Human Body Models, *Elemance*. [Online]. Available: http://www.elemance.com/virtual-human-body-models/. [Accessed: 26-Nov-2018].
[26] Iraeus, J , Brolin, K , Pipkorn, B, Generic finite element models of human ribs, developed and validated for stiffness and strain prediction – To be used in rib fracture risk evaluation for the human population in vehicle crashes, *Journal of the Mechanical Behavior of Biomedical Materials*, 2020, In Press:
[27] Pipkorn, B , Iraeus, J , Björklund, M , Bunketorp, O , Jakobsson, L, Multi-Scale Validation of a Rib Fracture Prediction Method for Human Body Models, Proceedings of *The International Research Council on Biomechanics of Injury (IRCOBI) Conference*, 2019.
[28] Kleiven, S, Predictors for Traumatic Brain Injuries Evaluated through Accident Reconstructions, *Stapp Car Crash Journal*, 2007, 51:81–114.
[29] Kleiven, S , Hardy, WN, Correlation of an FE Model of the Human Head with Local Brain Motion--Consequences for Injury Prediction., *Stapp Car Crash Journal*, 2002, 46:123–144.
[30] Gennarelli, TA , Thibault, LE , et al., Diffuse Axonal Injury and Traumatic Coma in the Primate, *Annals of Neurology*, 1982, 12(6):564–574.
[31] Galbraith, J a , Thibault, LE , Matteson, DR, Mechanical and Electrical Responses of the Squid Giant Axon to Simple Elongation, *Journal of Biomechanical Engineering*, 1993, 115(1):13–22.
[32] Bain, AC , Meaney, DF, Tissue-Level Thresholds for Axonal Damage in an Nervous System White Matter Injury, *Journal of Biomechanical Engineering*, 2000, 122(6):615–622.
[33] Morrison, B , Cater, HL , et al., A Tissue Level Tolerance Criterion for Living Brain Developed with an In Vitro Model of Traumatic Mechanical Loading, *Stapp Car Crash Journal*, 2003, 47:93–105.
[34] Shreiber, D , Bain, A , Meaney, D, In Vivo Thresholds for Mechanical Injury to the Blood-Brain Barrier, Proceedings of *Proceedings of the 41 Stapp Car Crash Conference*, 1997.
[35] Holbourn, AHS, Mechanics of Head Injuries, *The Lancet*, 1943, 242(6267):438–441.
[36] Hirsch, AE , Ommaya, AK, Protection From Brain Injury - The Relative Significance of Translational and Rotational Motions of the Head After Impact, Proceedings of *Proceedings of the 14th Stapp Car Crash Conference*, 1970.
[37] Gennarelli, TA , Thibault, LE , Ommaya, AK, Pathophysiologic Responses to Rotational and Translational Accelerations of the Head, Proceedings of *Proceedings of the 16th Stapp Car Crash Conference*, 1972.
[38] Wei, J , Dharani, LR, Response of Laminated Architectural Glazing Subjected to Blast Loading, *International Journal of Impact Engineering*, 2006, 32(12):2032–2047.
[39] Zhang, X , Hao, H , Ma, G, Parametric Study of Laminated Glass Window Response to Blast Loads, *Engineering Structures*, 2013, 56:1707–1717.
[40] Bennison, SJ , Jagota, A , Smith, CA, Fracture of Glass/Poly (Vinyl Butyral) (Butacite®) Laminates in Biaxial Flexure, *Journal of the American Ceramic Society*, 1999, 82(7):1761–1770.
[41] Thompson, GM , Kilgur, A, Detailed Windscreen Model for Pedestrian Head Impact, Proceedings of

Proceedings of the 9th LS-DYNA Forum, 2010.
[42] Sun, D , Andrieux, F, Modelling of the Failure Behaviour of Windscreens and Component Tests, Proceedings of *Proceedings of the LS-DYNA User Conference*, 2005.
[43] Alvarez, VS , Kleiven, S, Importance of Windscreen Modelling Approach for Head Injury Prediction, Proceedings of *Proceedings of the International Research Council on Biomechanics of Injury (IRCOBI) Conference*, 2016.
[44] Hardy, RN , Watson, JW , et al., Impact conditions for pedestrians and cyclists - APROSYS Deliverable D3.2.3, 2004.
[45] Singh, H , Kan, C-D , Marzougui, D , Morgan, R, Update to Future Midsize Lightweight Vehicle Findings in Response to Manufacturer Review and IIHS Small-Overlap Testing, 2016.
[46] Trotta, A , Ní Annaidh, A , Burek, RO , Pelgrims, B , Ivens, J, Evaluation of the head-helmet sliding properties in an impact test, *Journal of Biomechanics*, 2018, 75:28–34.
[47] Takhounts, EG , Craig, MJ , Moorhouse, K , McFadden, J , Hasija, V, Development of Brain Injury Criteria (BrIC), *Stapp Car Crash Journal*, 2013, 57:243–266.
[48] Final economic assessment; FMVSS No. 201 Upper interior head protection, Washington, DC: U.S. Department of Transportation, 1995.
[49] Patton, D , McIntosh, S , Kleiven, S , Frechede, B, Injury data from unhelmeted football head impacts evaluated against critical strain tolerance curves, *Journal of Sports Engineering and Technology*, 2012, 226:177–184.
[50] EuroNCAP, European New Car Assessment Programme - Pedestrian Testing Protocol, 2014.
[51] Katsuhara, T , Miyazaki, H , Kitagawa, Y , Yasuki, T, Impact kinematics of cyclist and head injury mechanism in car-to-bicycle collision, *2014 IRCOBI Conference Proceedings - International Research Council on the Biomechanics of Injury*, 2014, 670–684.
[52] Kleiven, S, Why Most Traumatic Brain Injuries are Not Caused by Linear Acceleration but Skull Fractures are, *Frontiers in Bioengineering and Biotechnology*, 2013, 1(November):1–5.
[53] Klein, KS , Thompson, D , Scheidt, PC , Overpeck, MD , Gross, LA, Factors associated with bicycle helmet use among young adolescents in a multinational sample, *Injury Prevention*, 2005, 11(5):288–293.
[54] Alvarez, VS , Halldin, P , Kleiven, S, The Influence of Neck Muscle Tonus and Posture on Brain Tissue Strain in Pedestrian Head Impacts, *Stapp Car Crash Journal*, 2014, 58(November):63–101.
[55] Iwamoto, M , Nakahira, Y, A Preliminary Study to Investigate Muscular Effects for Pedestrian Kinematics and Injuries Using Active THUMS, Proceedings of *Proceedings of the International Research Council on Biomechanics of Injury (IRCOBI) Conference*, 2014, 81(561):.
[56] AS/NZS 2063:2008, Australian / New Zealand Standard - Bicycle Helmets, 2008, .
[57] Consumer Product Safety Commision (CPSC), Safety Standard for Bicycle Helmets; Final Rule, *Federal Registry*, 1998, 63(46):11711–11747.
[58] European Committee for Standardization EN1078, Helmets for Pedal Cyclists and for Users of Skateboards and Roller Skates. EN1078:2012, 2012.
[59] Rizzi, MC , Rizzi, M , Kullgren, A , Algurén, B, The potential of different countermeasures to prevent injuries with high risk of health loss among bicyclists in Sweden, *Traffic Injury Prevention*, 2020, In press:1–7.
[60] Ohlin, M , Strandroth, J , Tingvall, C, The combined effect of vehicle frontal design, speed reduction, autonomous emergency braking and helmet use in reducing real life bicycle injuries, *Safety Science*, 2017, 92:338–344.

VIII. APPENDIX

Appendix A - SAFER HBM v9 Modifications to the THUMS v3 model

TABLE AI
SAFER HBM v9 Modifications to the THUMS v3 model

Body Part		Modification
Chest	**Ribs**	**Geometry and mesh modified** Shi, X., Cao, L., Reed, M. P., Rupp, J. D., Hoff, C. N., Hu, J. (2014) A statistical human rib cage geometry model accounting for variations by age, sex, stature and body mass index. *Journal of Biomechanics,* **47**(10): pp. 2277–85. **Cortical bone thickness modified** Choi, H-Y, Kwak, D-S (2011) Morphologic Characteristics of Korean Elderly Rib. *Journal of Automotive Safety and Energy*, **2**. **Cortical bone properties modified** Kemper, A. R., *et al*. (2005) Material properties of human rib cortical bone from dynamic tension coupon testing. *Stapp Car Crash Journal,* **49**: pp. 199–230. Kemper, A. R., *et al*. (2007) The biomechanics of human ribs: material and structural properties from dynamic tension and bending tests. *Stapp Car Crash Journal,* **51**: pp. 235–73.
	Sternum	**Geometry and mesh modified** 50^{th} percentile male sternum Weaver, A. A., Schoell, S. L., Nguyen, C. M., Lynch, S. K., Stitzel, J. D. (2014) Morphometric analysis of variation in the sternum with sex and age. *Journal of Morphology,* **275**(11): pp. 1284–99.
Lumbar Spine	**Vertebra**	**Remeshed** Contact between vertebra and intervertebral disc added Intervertebral ligaments modified – both geometry and properties Afwerki, H. (2016) Biofidelity Evaluation of Thoracolumbar Spine Model in THUMS. Master's Thesis in Biomedical Engineering, Chalmers University of Technology, 2016.
Head		**KTH FE Head Model** Kleiven, S. (2007) Predictors for Traumatic Brain Injuries Evaluated through Accident Reconstructions. *Stapp Car Crash Journal,* **51**: pp. 81–114.

Appendix B - The KTH FE Head Model

The head model includes the scalp, the skull, the brain, the meninges, the cerebrospinal fluid (CSF) and eleven pairs of the largest parasagittal bridging veins, see Fig. 11, with material properties adapted from the study by [27] listed in TABLE II. To accommodate large elastic deformations of the brain, a second order Ogden hyperelastic constitutive model was used together with a linear viscoelastic model. The constitutive constants used for the brain tissue are also adapted from [27] and presented in TABLE V.

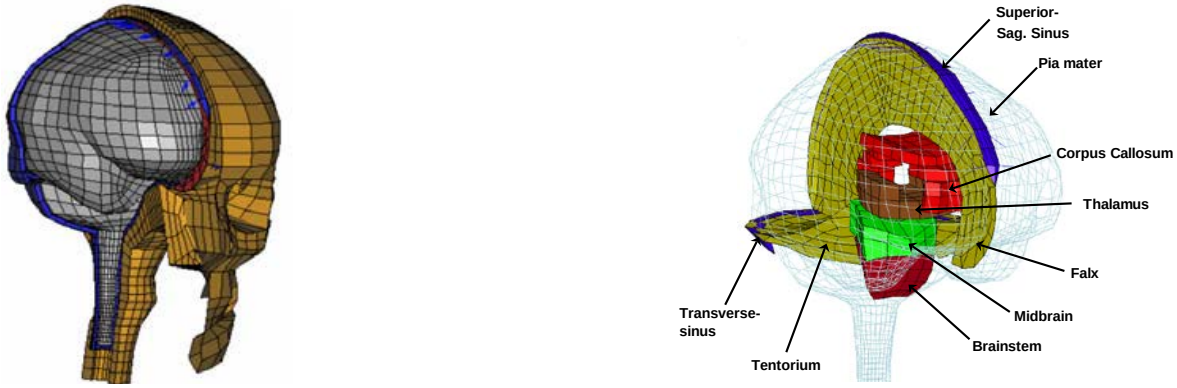

Fig. B1. Finite element model of the human head [27].

TABLE BI
MATERIAL PROPERTIES USED FOR THE FE HEAD MODEL

Tissue	Young's modulus [MPa]	Density [kg/dm^3]	Poisson's ratio
Outer compact bone	15 000	2.00	0.22
Inner compact bone	15 000	2.00	0.22
Porous bone	1000	1.30	0.24
Brain	Hyper-Viscoelastic	1.04	0.49999
Cerebrospinal Fluid	K = 2.1 GPa	1.00	-
Sinuses	K = 2.1 GPa	1.00	-
Dura mater	31.5	1.13	0.45
Falx/Tentorium	31.5	1.13	0.45
Pia mater	11.5	1.13	0.45
Scalp	Hyper-Viscoelastic	1.13	0.42
Bridging veins	EA = 1.9 N		

K = Bulk modulus, and EA = Force/unit strain.

TABLE BII
OGDEN HYPERELASTIC AND LINEAR VISCOELASTIC CONSTANTS

Parameter	Value
μ_1 (Pa)	53.8
μ_2 (Pa)	-120.4
α_1	10.1
α_2	-12.9
G_1 *(MPa)*	0.32
G_2 *(kPa)*	78
G_3 *(kPa)*	6.2
G_4 *(kPa)*	8.0
G_5 *(kPa)*	1.0
G_6 *(kPa)*	3.0
β_1 (1/s)	10^6
β_2 (1/s)	10^5
.	
.	
β_6 (1/s)	10^1

Appendix C - Images at time of head impact for all impact configurations

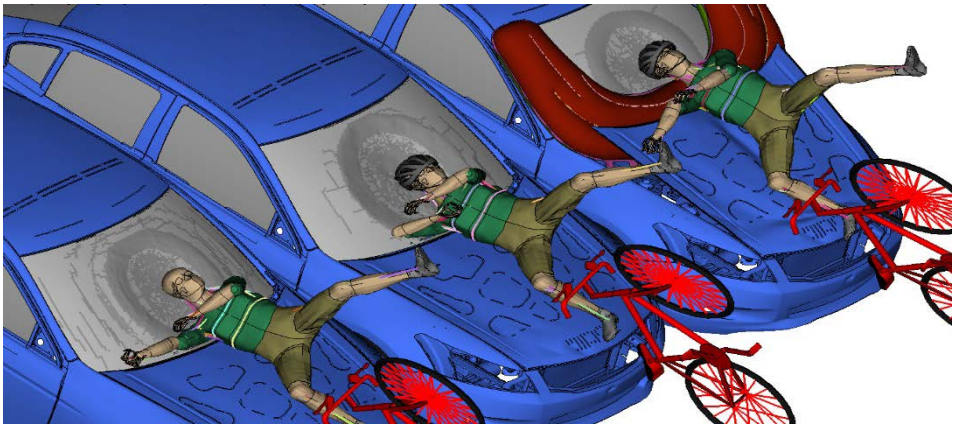

Fig. C1. Snapshots from impact between vehicle velocity 40km/h and stationary bicyclist at time of head impact.

Fig. C2. Snapshots from impact between vehicle velocity 40km/h and bicyclist moving in 15km/h, at time of head impact.

Appendix D - Head CG relative velocity time histories

Fig.s D1 and D2 shows the resultant linear head velocity relative to the impacting vehicle as a function of time.

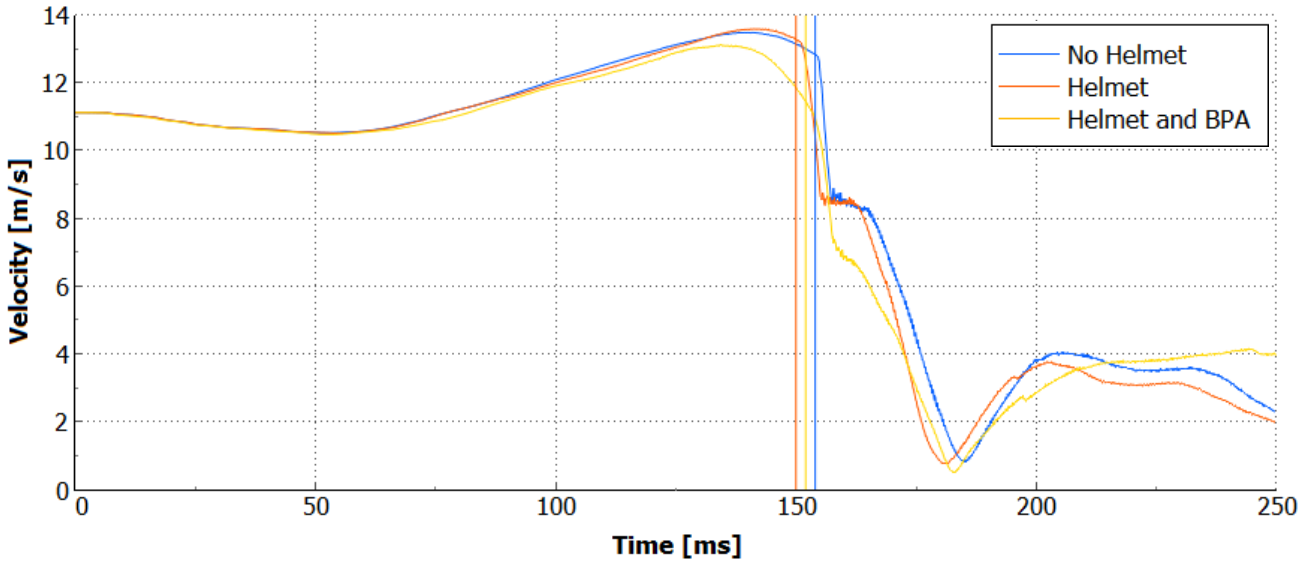

Fig. D1. Head CG relative velocity at vehicle velocity 40km/h and stationary bicyclist. Vertical lines indicate time of head impact for respective simulation.

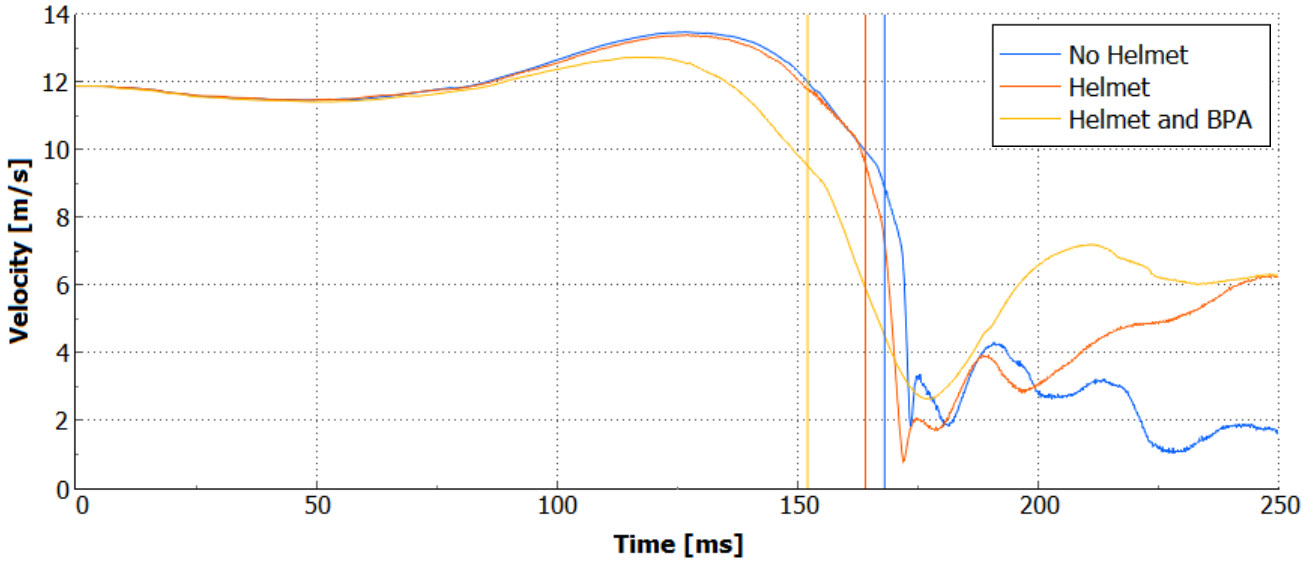

Fig. D2. Head CG relative velocity at vehicle velocity 40km/h and 15km/h bicycle velocity. Vertical lines indicate time of head impact for respective simulation.

Appendix E - Head CG Angular velocity time histories

In Fig.s E1 and E2 the head CG angular velocity is plotted for each component in local coordinate system according to the SEA standard convention.

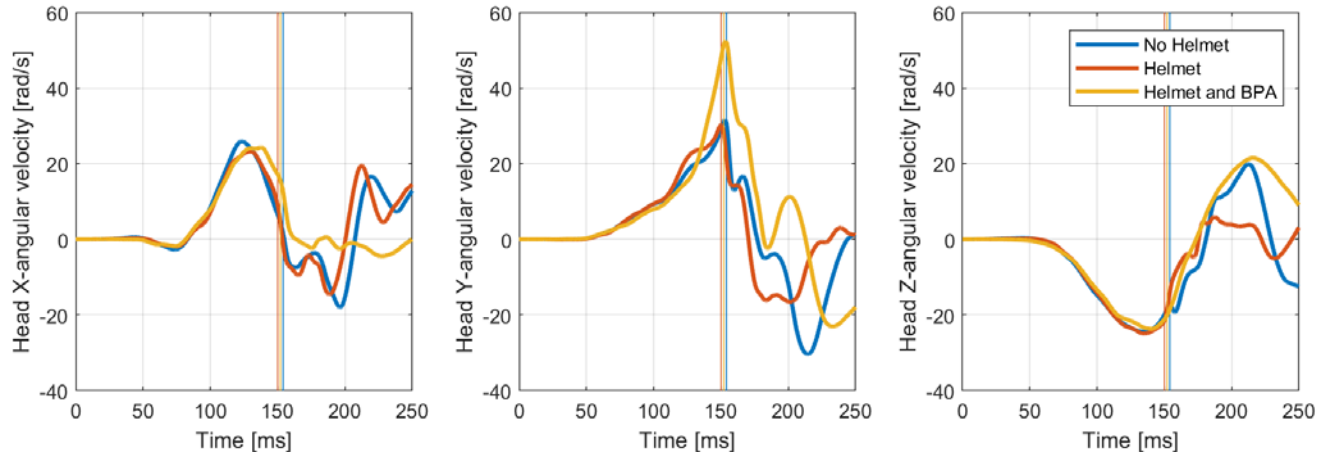

Fig. E1. Head CG angular velocity at vehicle velocity 40km/h and stationary bicyclist. Vertical lines indicate time of head impact for respective simulation.

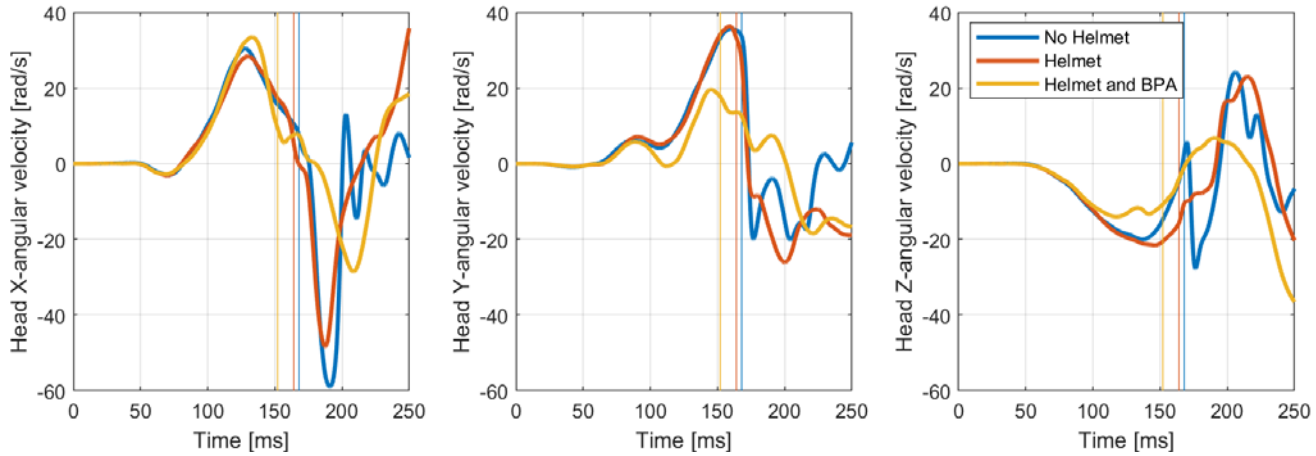

Fig. E2. Head CG angular velocity at vehicle velocity 40km/h and 15km/h bicycle velocity. Vertical lines indicate time of head impact for respective simulation.

Appendix F - Strain in the brain time histories

Fig.s F1-F3 shows the maximum strain in the brain as function of time for all impact configurations.

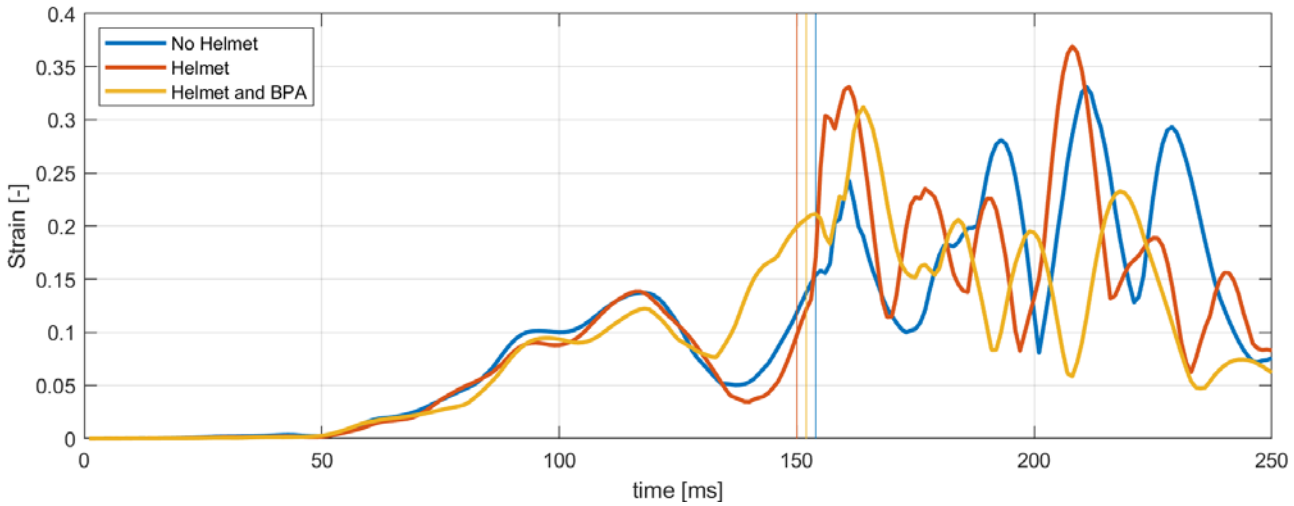

Fig. F1. Maximum strain in the brain at vehicle velocity 40km/h and stationary bicyclist. Vertical lines indicate time of head impact for respective simulation.

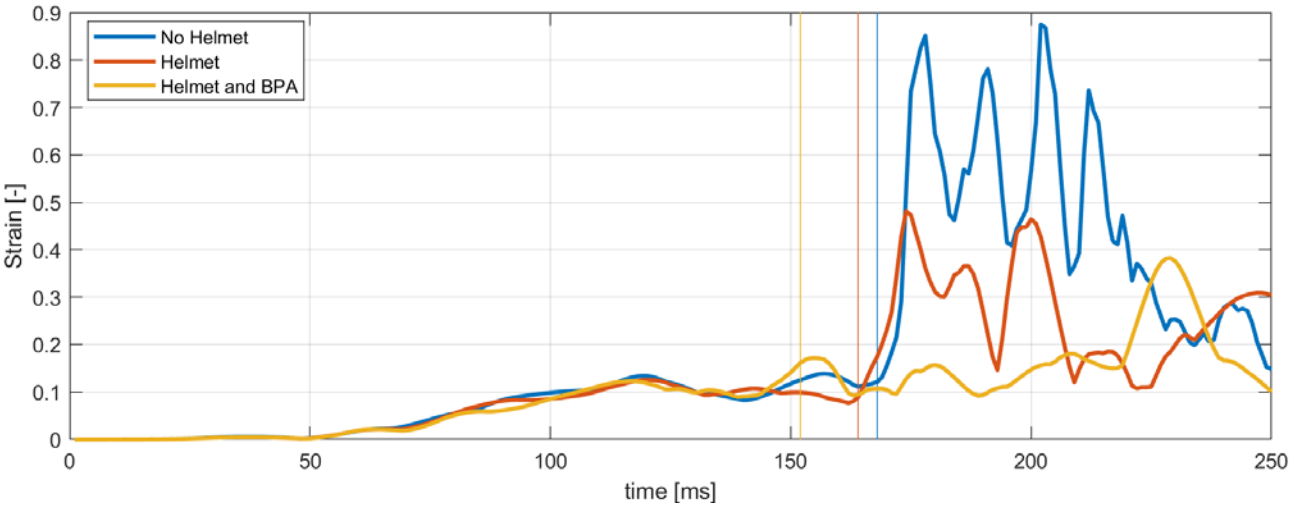

Fig. F2. Maximum strain in the brain at vehicle velocity 40km/h and 15km/h bicycle velocity. Vertical lines indicate time of head impact for respective simulation.

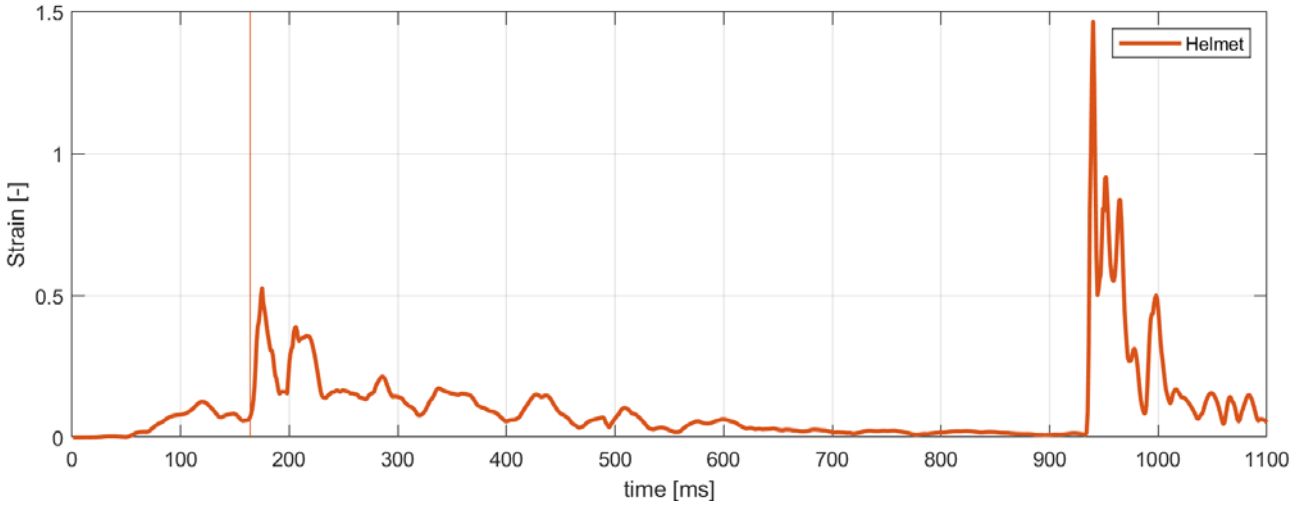

Fig. F3. Maximum strain in the brain at vehicle velocity 40km/h and 15km/h bicycle velocity for simulation including ground impact. Vertical line indicates time of head impact towards vehicle.